Supplementary Information for

Transforming $Ti_3C_2T_x$ MXene into nanoscale ionic materials via an electronic interaciton strategy

Dechao Wang[a], Hailong Ning[b], Yangyang Xin[a], Yudeng Wang[a], Xiaoqian Li[a], Dongdong Yao[a, *], Yaping Zheng[a, *], Yuting Pan[c], Hongmin Zhang[a], Zhongjie He[a], Chen Liu[a], Menglan Qin[a], Zehao Wang[a], Ruilu Yang[d], Peipei Li[e], Zhiyuan Yang[b, f, *]

[a] School of Chemistry and Chemical Engineering, Northwestern Polytechnical University, Xi'an 710129, P. R. China

[b] College of Chemistry and Chemical Engineering, Xi'an University of Science and Technology, Xi'an 710021, P. R. China

[c] Queen Mary University of London Engineering School, Northwestern Polytechnical University, Xi'an 710129, Shaanxi, P. R. China

[d] Analysis and Testing Center, Nantong University, Nantong, Jiangsu, 226019, P. R. China

[e] School of Advanced Materials and Nanotechnology, Xidian University, Xi'an, Shaanxi, 710071, P. R. China

[f] Key Laboratory of Coal Resources Exploration and Comprehensive Utilization, Ministry of Natural Resources, Xi'an 710021, P. R. China

*Corresponding authors. E-mail: yaodd@nwpu.edu.cn (Dongdong Yao); zhengyp@nwpu.edu.cn (Yaping Zheng); zhiyuanyang@126.com (Zhiyuan Yang)

Table of Contents

1. Experimental sections

1.1 Preparation of membranes

A drop-casting technique was used to prepare MMMs. Briefly, a certain amount of Pebax-1657 pellets was dissolved in mixture (ethanol/ water (70/30 by weight)) and stirred for 4 h at 80°C to obtain 4.0 wt% of Pebax-1657 solution. Next, a certain amount of MX-I-M2070 were mixed with Pebax-1657 solution under ultrasonic condition and stirred continuously for 8 h. Afterward, the above mixed solution was poured into an ultra-flat petri dish, left for 12 h at 25°C and 45°C for 48 h, respectively. After this period, MMMs were successfully obtained. The resultant MMMs were abbreviated as Pebax/MX-I-M2070-X, where P represents Pebax-1657, X represents the filler content of MX-I-M2070. The thickness of membranes was controlled within 80~130 μm. By contrast, the pristine Pebax-1657 membrane was also prepared following the same procedure without MX-I-M2070.

1.2. Gas uptake measurement

The schematic diagram of high-temperature and high-pressure adsorption instrument analyzer is shown in Fig. S5. The adsorption test principle is summarized as follows: First, the testing parameters setting (testing temperature and testing pressure) are completed. Then, the evacuation value is opened by the automatic control system and the target gas enters the reference cavity. When the pressure reaches the set value, the pressure P_1 of reference cavity is recorded. Next, the valve V_1 is opened, the target gas enters into the sample cell and is absorbed by the sample. When the adsorption equilibrium is achieved, the pressure P_2 of reference cavity is recorded. The equilibrium adsorption capacity is analyzed and recorded according to the pressure change of reference cavity by the automatic control and data recording system.

1.3. Gas separation evaluation

In this study, a circular membrane with effective area of 38.48 cm^2 was used for measurement. The membrane thickness was in the range of 80~130 μm. The values of

permeability and selectivity were calculated for 3 different membranes for MMMs with same filler addition under the same testing conditions.

1.4. Breakthrough curves testing

The measurement of breakthrough curve involved the following steps: (1) Regeneration of adsorption column: evacuate the equipment adsorption column for more than 1 h, then nitrogen was passed into column until the pressure reached 300 KPa. (2) Measurement of the breakthrough curve: allowed for 15% volume faction CO_2 balanced by 85% N_2 at 100 $mL \cdot min^{-1}$, meanwhile the adsorption column outlet valve was opened. The flow was controlled through the outlet valve until methane fully penetrated the column bed. During the adsorption stage, the outlet CO_2 volume concentration was monitored by a fixed methane concentration detector as a function of time (breakthrough curve), and breakthrough data was transferred to a computer. In the inlet and outlet of the column, solenoid valve was set up and the automatic control was realized *via* a program control panel. Breakthrough time defined as the time it takes for CO_2 detection at the outlet adsorption column, when the outlet CO_2 volume fraction reached 1.25 Vol%.

2. Molecular Simulations

The molecular simulations was performed using Material Studio (7.0) package (*Accelrys Software Inc*). The purpose is to investigate the adsorption density filed distribution of CO_2 and N_2 in MX-I-M2070 using Grand Canonical Monte Carlo (GCMC) method [1], which can reveal the selective separation potential.

2.1 Molecular Structures Construction

In the beginning, molecular models of oligomer species, $Ti_3C_2T_x$ MXene and independent MX-I-M2070 were constructed using *Amorphous Cell module*. Then, the constructed MX-I-M2070 was subjected to geometry optimization and following structural relaxation via annealing process. Finally, the obtained low-energy configurations were further optimized by *5*00-*ps* NVT molecular dynamics (MD) and 200-*ps* NPT MD to monitor the

fluctuation of density. Afterward, the obtained optimum structure was used to construct membrane models in the following procedures.

Next, the model of MX-I-M2070 was constructed using *Amorphous Cell* module. All these cells with cubic form were built with 5 output frames and the initial density was set on 0.2 g/cm^3 at 298 K [2]. Then, all of amorphous cells were optimized via geometry optimization. The local energy was minimized by the method of smart minimizer. During the minimization, convergence level was set to 0.0001 kcal/mol/Å. Subsequently, the obtained lowest energy configurations were all subjected to annealing process, in which temperature was increased from 298 K to 600 K. The highest temperature is well above the glass transition temperature (T_g) of oligomer species. And then it was cooled back at intervals of 5℃ at each step in which 200-*ps* NVT dynamics was carried out. Thereafter, a 500-*ps* MD simulation in an NVT ensemble was done to relax the structure, in which time step was 1 fs and Nose thermostat were utilized [3]. The equations of motion were integrated by velocity Verlet algorithm with a time step of 1 fs for all simulation runs. The electrostatic interactions were calculated by the Atom based method with accuracy of 0.0001 kcal/mol.

2.2 Force Fields

Force field parameters of oligomer species were based on COMPASS [4]. The $Ti_3C_2T_x$ MXene were treated as a rigid framework and the Lennard-Jones parameters were adopted using the universal force field. Atomic charges for $Ti_3C_2T_x$ MXene were obtained using the Rappe-Goddard charge equilibration method (QEq) [5].

2.3 Grand Canonical Monte Carlo (GCMC) simulation

The GCMC simulation is a powerful method to analyze the loading-dependent gas adsorption or transport [6, 7]. In this ensemble, temperature T, volume V and chemical potential μ were fixed, while the number of particles N was allowed to be determined. To be specific, the related algorithm generates a serious of ‘moves’ that are accepted or rejected according to the following probabilities:

$$P = \exp\left(-\frac{E}{k_B T}\right)\frac{fV_{box}}{(N+1)k_B T} \quad \text{(creation)} \quad (1)$$

$$\Pr obability = \exp\left(-\frac{E}{k_B T}\right)\frac{Nk_B T}{fV_{box}} \quad \text{(deletion)} \quad (2)$$

$$\Pr obability = \exp\left(-\frac{E_1 - E_2}{RT}\right) \quad \text{(displacement or rotation)} \quad (3)$$

where E is the potential energy, f is the fugacity, and k_B is the Boltzmann constant.

In present simulation process, the well-known Metropolis algorithm is used to accept or reject a configurational move of gas molecules. The Berendsen thermostat was used for temperature monitoring. 1000000 steps of GCMC calculations were carried out with the initial equilibration period of 100000 steps [8]. To simulate the sorption in the process of gas penetration into porous liquids, tasks of adsorption isotherm and fixed pressure were performed, respectively. The adsorption density filed distribution of CO_2 molecular in NIMs was analyzed according to adsorption behavior at 10.0 bar.

2.4 Fractional Accessible Volume (FAV) Analysis

The fractional accessible volume (FAV) is the locus of the probe centre as the probe freely rolls over the framework. A gas molecule probe is randomly inserted into simulation box and the insertion is considered to be successful if the probe does not overlap with any polymer atom. In the calculation process, N_2 molecule was chosen as the molecule probe. The ratio of successful insertion to the total number of insertion gives FAV. Therefore, it is a reasonable method to determine the changes of free accessible volume. In this study, FAV for constructed cells were obtained using the “connolly surface” from the Visualizer module.

3. Data Analysis

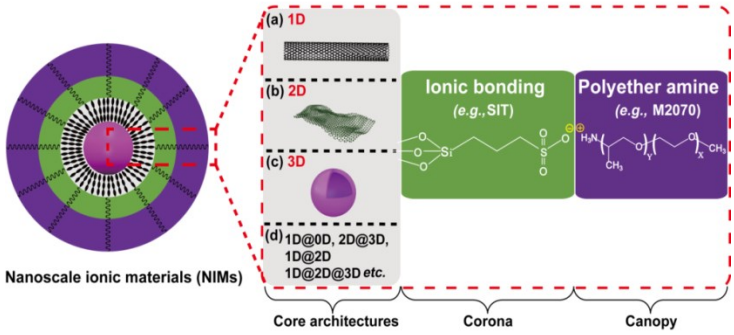

Fig. S1 The structure illustration for a representative structure of NIMs.

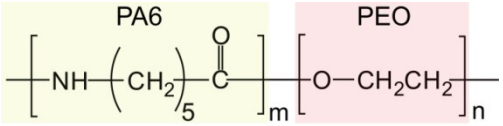

Fig. S2 The chemical structure of Pebax-1657 (the weight ratio of PA6 to PEO (x:y) is 40:60)

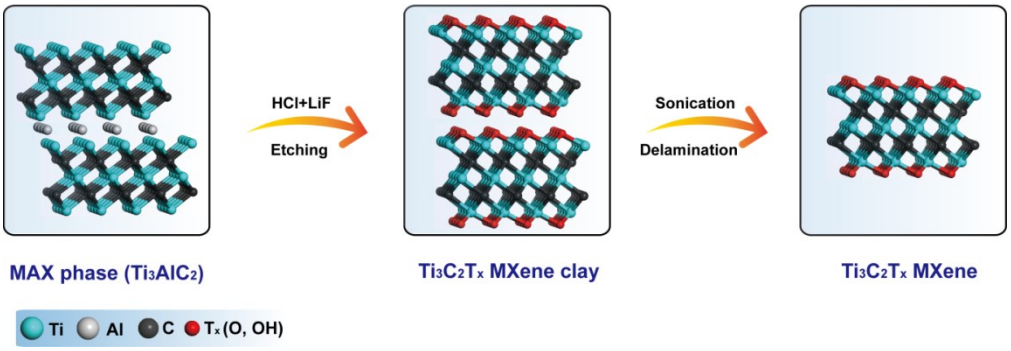

Fig. S3 Synthesis of $Ti_3C_2T_x$ MXene.

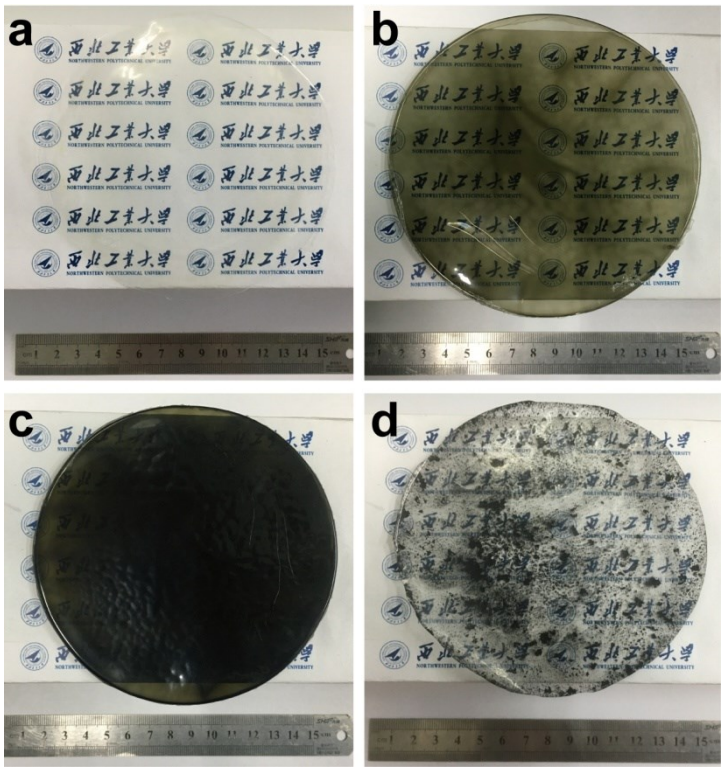

Fig. S4 Digital photographs of as-prepared MMMs. (a) Pure Pebax-1657 membrane, (b) P-MX-fluid-(20), (c) P-MX-fluid-(80) and (d) P-MX-(1).

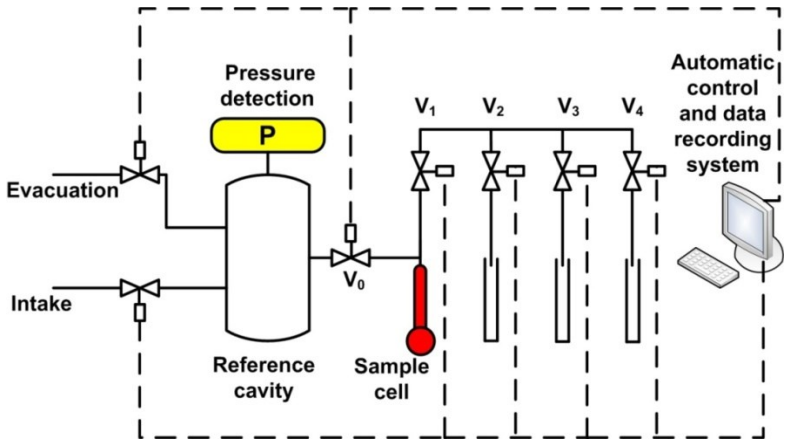

Fig. S5 Schematic diagram of the high-temperature and high-pressure adsorption instrument analyzer: V_0: pressure test valve; V_1: desorption valve; V_2: free valve; V_3: desorption collection valve; V_4: exhaust valve.

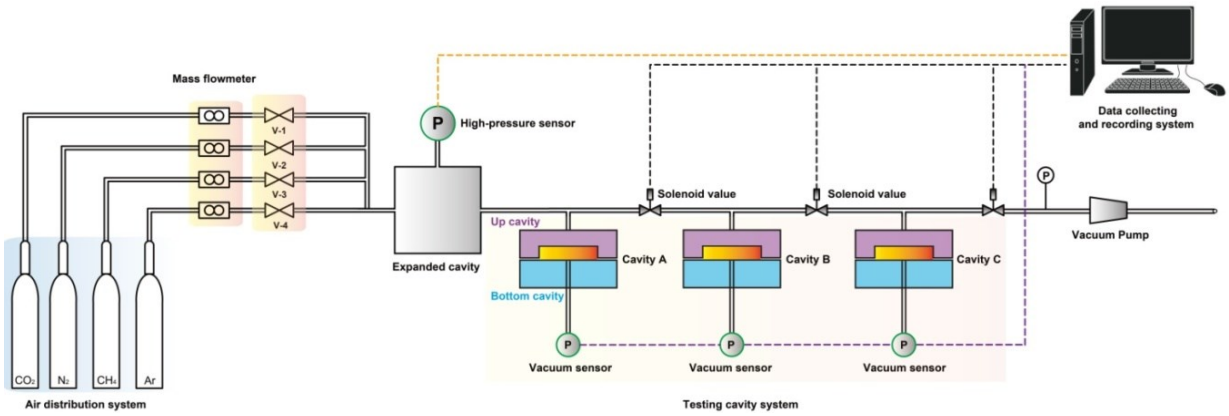

Fig. S6 Schematic diagram of gas permeation testing instrument.

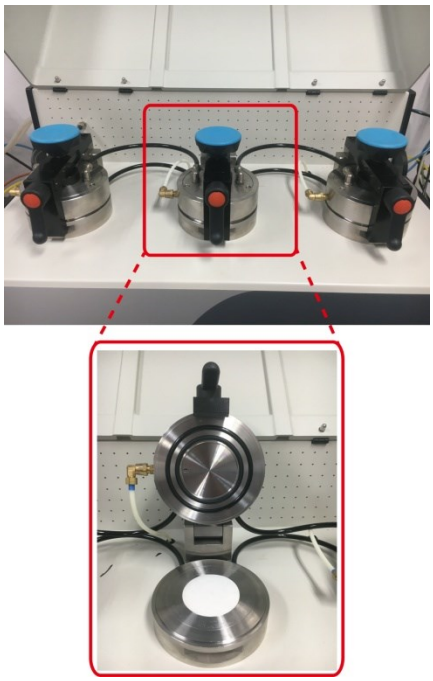

Fig. S7 Digital photos of gas permeation testing cavities.

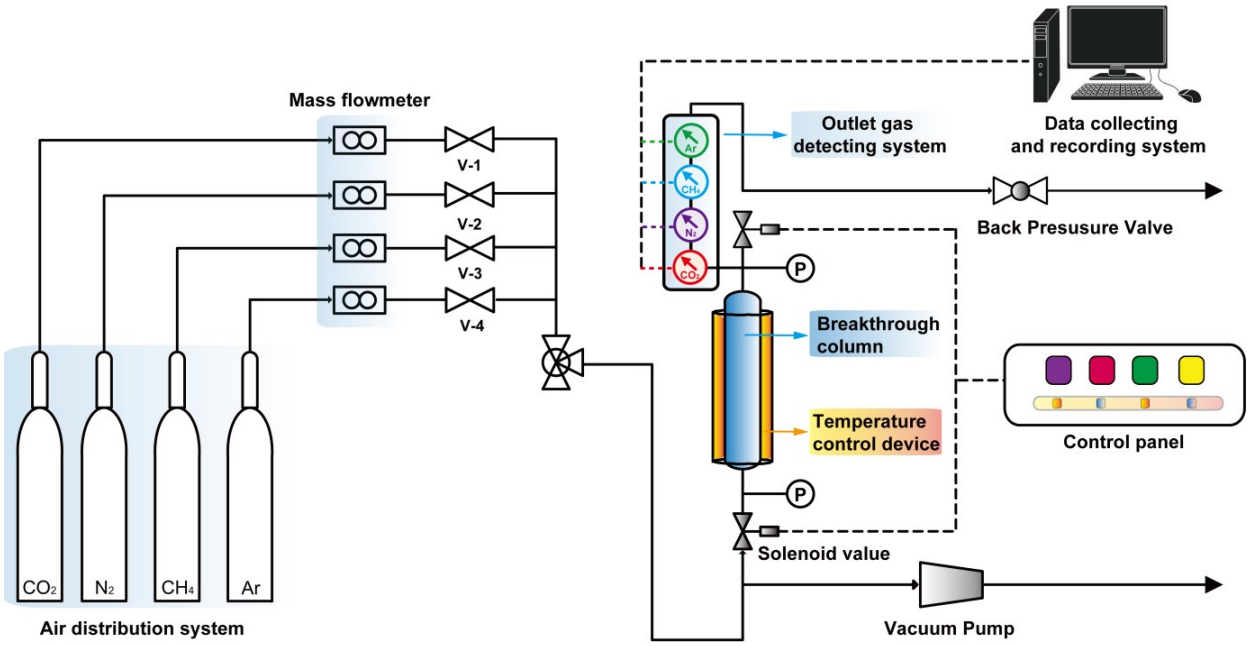

Fig. S8 Schematic diagram of installation for breakthrough curve experiments.

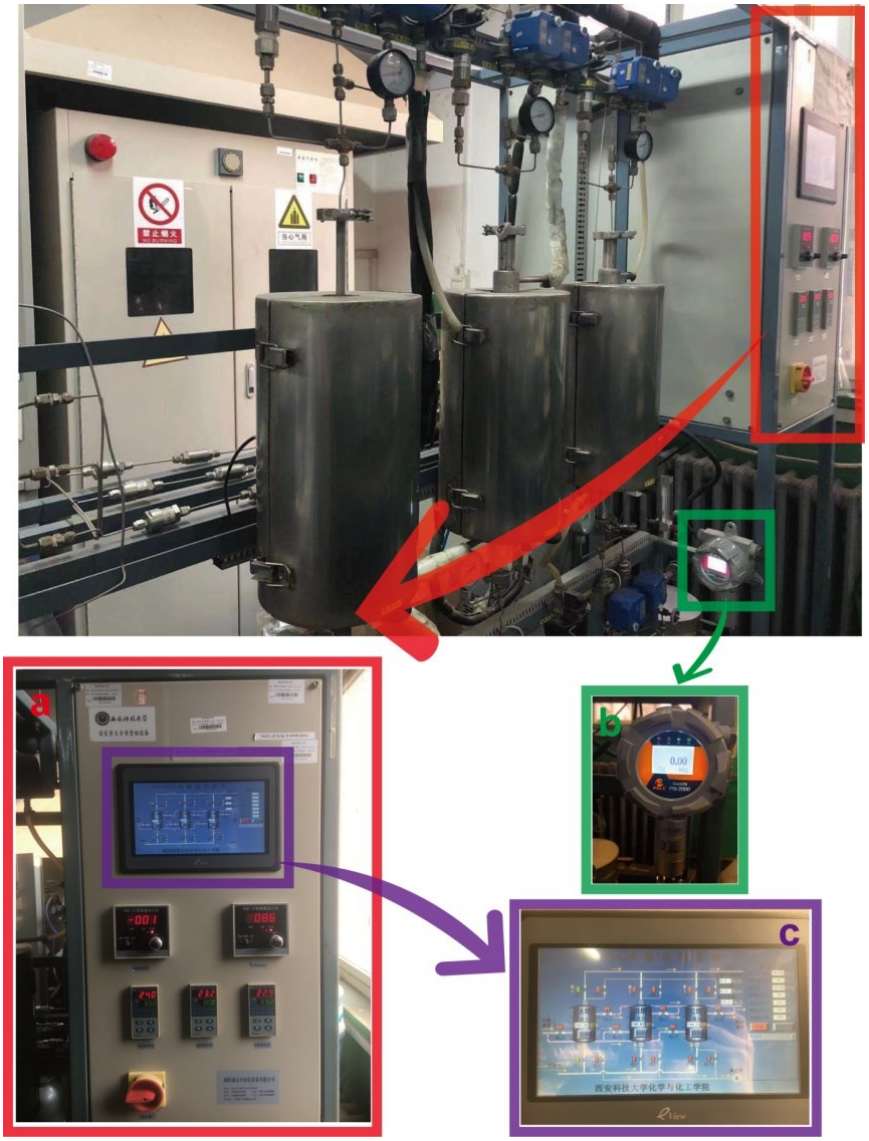

Fig. S9 The physical images of breakthrough curve experiments, (a) The operation panel; (b) The on-line CO_2 detector; (c) Real time control and displaying module.

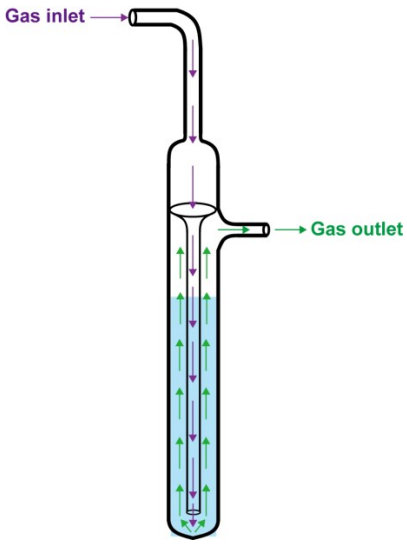

Fig. S10 Schematic representation of the breakthrough column loading with NIMs.

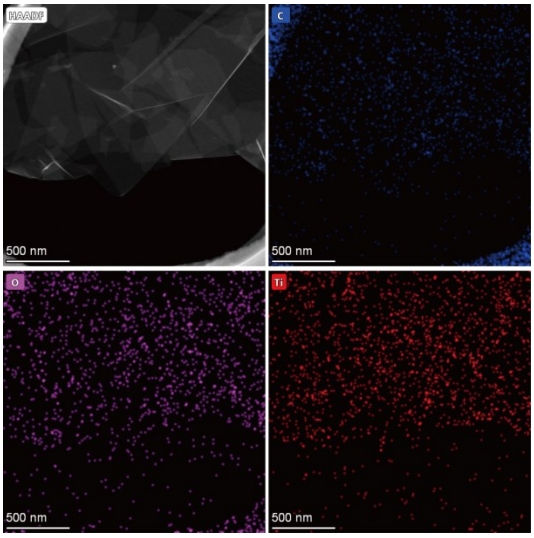

Fig. S11 The EDS mapping image of $Ti_3C_2T_x$ MXene.

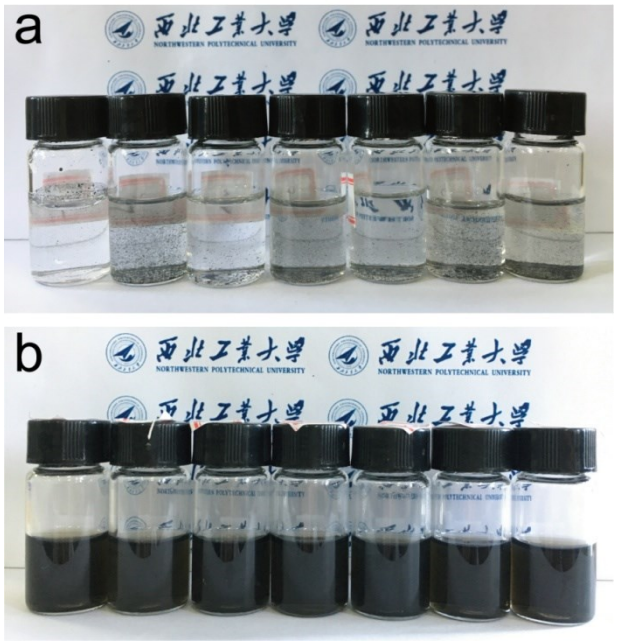

Fig. S12 Photos of (a) the pristine $Ti_3C_2T_x$ MXene after freeze drying and (b) MX-I-M2070 dispersed in various common solvents at a concentration of 20 mg·mL^{-1} after setting for two weeks. Storage conditions: Store in the air with cap on tight at room temperature. The solvents from left to right are as following: H_2O, ethanol, DMF, pyridine, chloroform, acetone and tetrahydrofuran (THF).

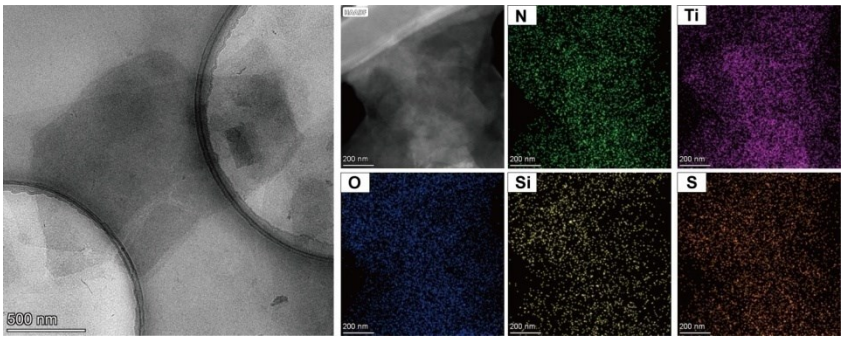

Fig. S13 TEM images of MX-I-M2070 after standing for 570 days.

Fig. S14 Squeezing MX-I-M2070 through a toothpick.

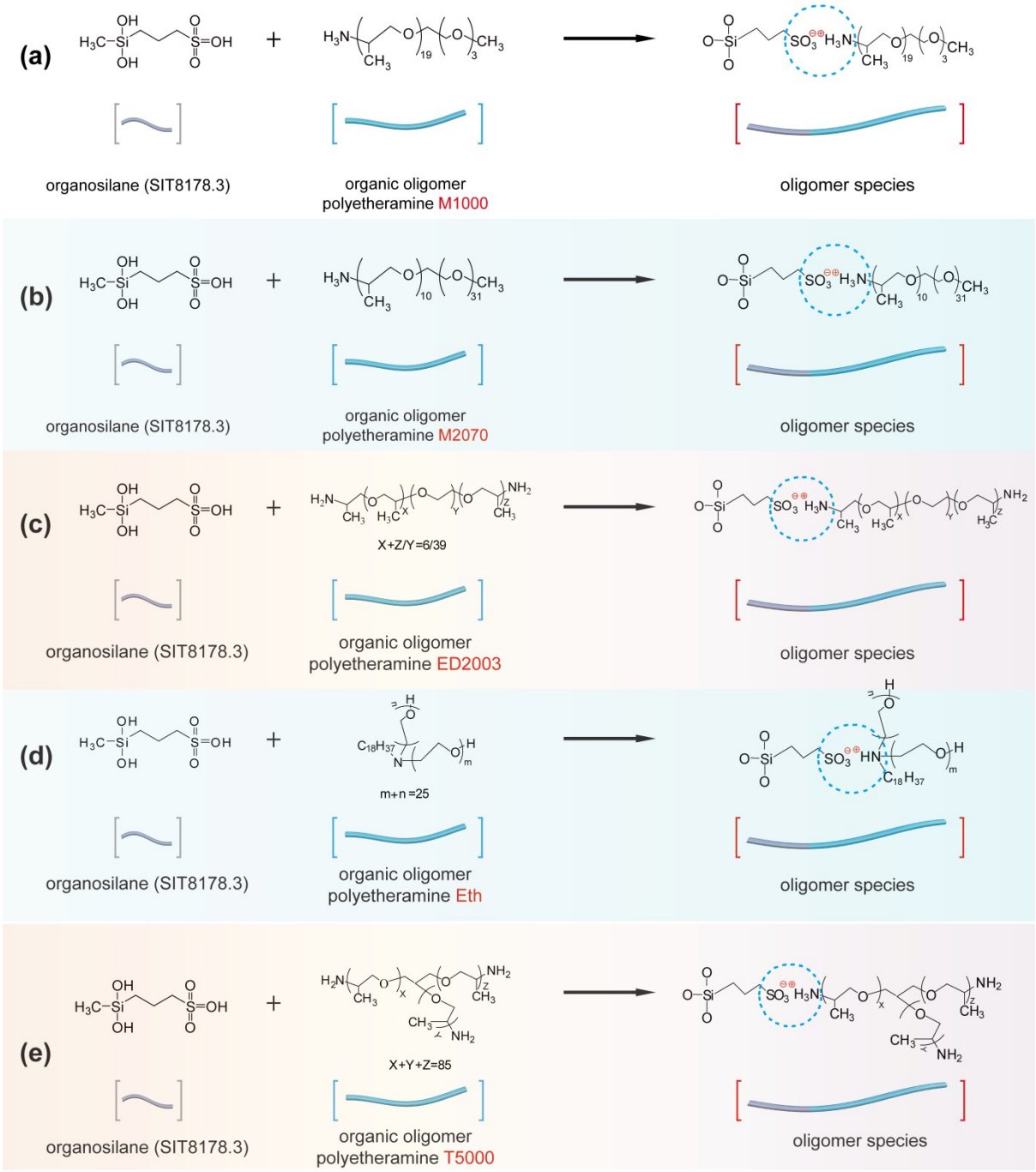

Fig. S15 The reactions of organosilane (OS) with acidic moieties, and different types of alkaline oligomers.

Fig. S16 Squeezing MX-I-M1000 through a toothpick.

Fig. S17 Squeezing MX-I-Eth through a toothpick.

Fig. S18 Squeezing MX-I-ED2003 through a toothpick.

Fig. S19 Squeezing MX-I-T5000 through a toothpick.

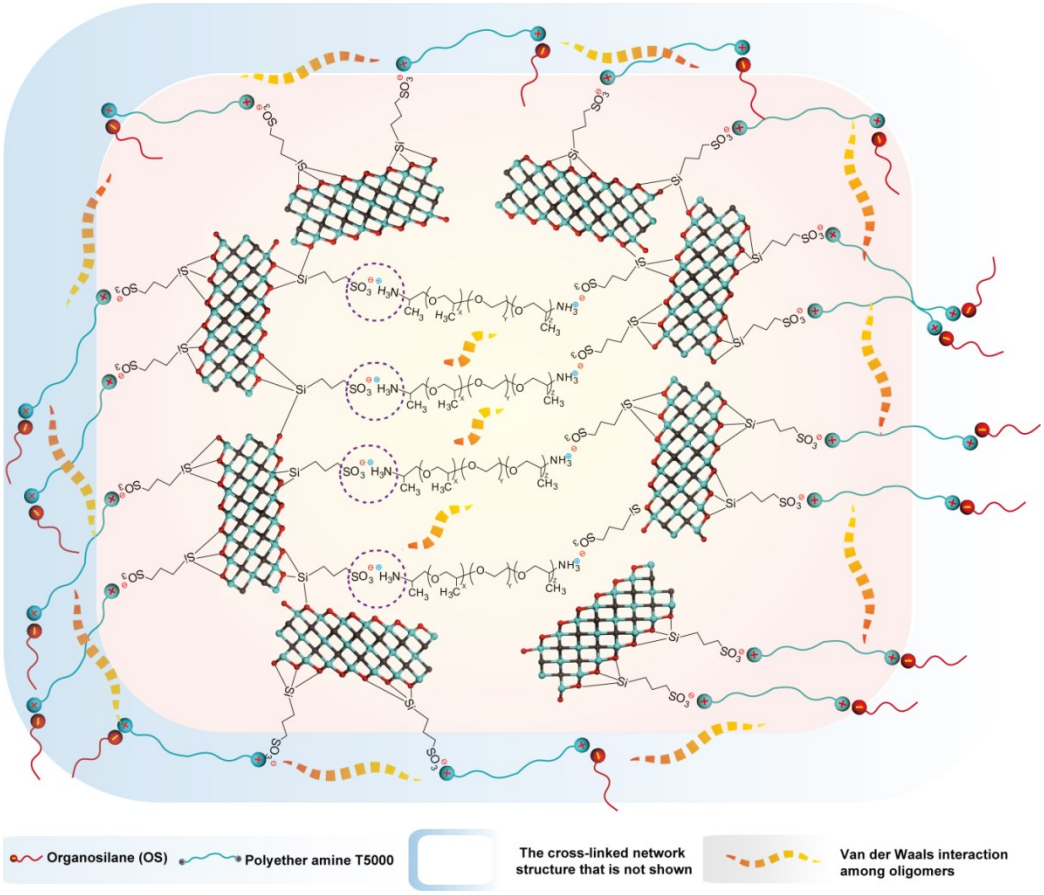

Fig. S20 Schematic of the bridging mechanism of MX-I-ED2003.

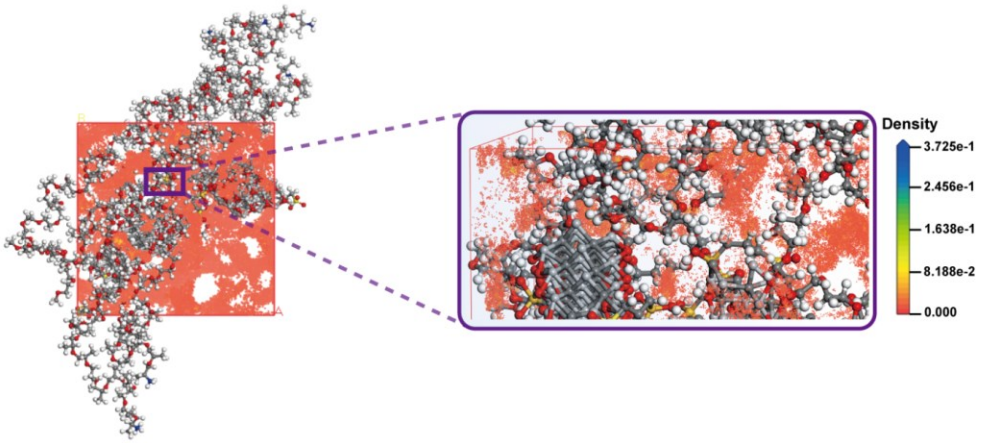

Fig. S21 The snapshot of showing N_2 adsorption in simulated MX-I-M2070 box using Grand Canonical Monte Carlo (GCMC) simulation.

Table S1 List of the structures of polyether amine canopy.

Polyether amine canopy	M1000	M2070	T5000	Eth	ED2003
M_w	1000	2070	5000	1470	2003
Amine types	Single-ended amine	Single-ended amine	Three-terminal amine	Tertiary amine	Double-ended amino
EO/PO	19/3	31/10	0/85	25/0	39/6

Table S2 Comparison of CO_2/N_2 separation performance between this work and previous reported MMMs with different classes of fillers under dry feed gas state.

Polymer	Filler	P(CO_2) / Barrer	α(CO_2/N_2)	Test conditions	Ref.
Pebax-1657	$CaCl_2$	35.6	49.7	25°C, 3.0 bar	[9]
Pebax-1657	CANs	85	55	25°C, 2.0 bar	[10]
Pebax-1657	ZIF-67	98.4	48.2	25°C, 2.0 bar	[11]
Pebax-1657	TiO_2	37.0	52.9	25°C, 4.0 bar	[12]
Pebax-1657	Attapulgite	77	52	35°C, 4.0 bar	[13]
Pebax-1657	CNTs	87	53	25°C, 2.0 bar	[14]
PEO-PBT	GO	143	73	25°C, 0.5 bar	[15]
PSF	CNTs	5.19	22.6	35°C, 4.0 bar	[16]
Pebax-1657	MX-I-M2070	91.9	58.2	25°C, 1.0 bar	This work

References

1 S. He, L. Chen, J. Cui, B. Yuan, H. Wang, F. Wang, Y. Yu, Y. Lee and T. Li, *J. Am. Chem. Soc.*, 2019. **141**, 19708-19714.

2 K. Golzar, S. Amjad-Iranagh, M. Amani and H. Modarress, *J. Membr. Sci.*, 2014. **451**, 117-134.

3 M. Pazirofteh, M. Dehghani, S. Niazi, A. H. Mohammadi and M. Asghari, *Journal of molecular liquids*, 2017. **241**, 646-653.

4 A. K. Rappe, C. J. Casewit, K. S. Colwell, W. A. Goddard and W. M. Skiff, *J. Am. Chem. Soc.*, 1992. **114**, 10024-10035.

5 A. K. Rappe, W. A. Goddard, *Journal of physical chemistry (1952)*, 1991. **95**, 3358-3363.

6 L. De Lorenzo, E. Tocci, A. Gugliuzza and E. Drioli, *J. Membr. Sci.*, 2012. **421-422**, 75-

84.

7 H. Bux, C. Chmelik, R. Krishna and J. Caro, *J. Membr. Sci.*, 2011. **369**, 284-289.

8 M. L. Connolly, *J. Am. Chem. Soc.*, 1985. **107**, 1118-1124.

9 W. Fam, J. Mansouri, H. Li, J. Hou and V. Chen, *Ind. Eng. Chem. Res.*, 2019. **58**, 3304-3313.

10 X. Li, Z. Jiang, Y. Wu, H. Zhang, Y. Cheng, R. Guo and H. Wu, *J. Membr. Sci.*, 2015. **495**, 72-80.

11 S. Feng, M. Bu, J. Pang, W. Fan, L. Fan, H. Zhao, G. Yang, H. Guo, G. Kong, H. Sun, Z. Kang and D. Sun, *J. Membr. Sci.*, 2020. **593**, 117404.

12 R. A. Zoppi, S. Das Neves and S. P. Nunes, *Polymer (Guilford)*, 2000. **41**, 5461-5470.

13 L. Xiang, Y. Pan, G. Zeng, J. Jiang, J. Chen and C. Wang, *J. Membr. Sci.*, 2016. **500**, 66-75.

14 X. Li, Y. Cheng, H. Zhang, S. Wang, Z. Jiang, R. Guo and H. Wu, *ACS Appl. Mater. Inter.*, 2015. **7**, 5528-5537.

15 M. Karunakaran, R. Shevate, M. Kumar and K. V. Peinemann, *Chem. Commun.*, 2015. **51**, 14187-14190.

16 S. Kim, L. Chen, J. K. Johnson and E. Marand, *J. Membr. Sci.*, 2007. **294**, 147-158.